Optical probe of Heisenberg-Kitaev magnetism in α-$RuCl_3$

Luke J. Sandilands,[1,2] C. H. Sohn,[1,2] H. J. Park,[1,2] So Yeun Kim,[1,2] K. W. Kim,[3] Jennifer A. Sears,[4] Young-June Kim,[4] and Tae Won Noh[1,2]

[1]*Center for Correlated Electron Systems, Institute for Basic Science, Seoul 08826, Republic of Korea*
[2]*Department of Physics and Astronomy, Seoul National University, Seoul 08826, Republic of Korea*
[3]*Department of Physics, Chungbuk National University, Cheongju, Chungbuk 28644, Republic of Korea*
[4]*Department of Physics and Center for Quantum Materials, University of Toronto, Toronto, Canada M5S 1A7*

(Received 16 March 2016; revised manuscript received 31 August 2016; published 30 November 2016)

We report a temperature-dependent optical spectroscopic study of the Heisenberg-Kitaev magnet α-$RuCl_3$. Our measurements reveal anomalies in the optical response near the magnetic ordering temperature. At higher temperatures, we observe a redistribution of spectral weight over a broad energy range that is associated with nearest-neighbor spin-spin correlations. This finding is consistent with highly frustrated magnetic interactions and in agreement with theoretical expectations for this class of material. The optical data also reveal significant electron-hole interaction effects, including a bound excitonic state. These results demonstrate a clear coupling between charge and spin degrees of freedom and provide insight into the properties of thermally disordered Heisenberg-Kitaev magnets.

DOI: 10.1103/PhysRevB.94.195156

I. INTRODUCTION

Identifying and understanding quantum spin liquid states, where quantum fluctuations preclude magnetic long-range order, is an important goal in condensed matter physics. Experimental progress has, however, been hindered by a scarcity of real materials displaying quantum spin liquid (QSL) behavior [1]. One possible avenue to realize such QSL states is in certain honeycomb lattice Mott insulators with strong spin-orbit coupling [2,3]. In these systems, the entanglement of spin and orbital degrees of freedom can lead to highly anisotropic, bond-directional interactions best described by an extended Heisenberg-Kitaev (HK) model [2–5]. For sufficiently strong Kitaev coupling K, a QSL ground state with fractionalized, Majorana fermion spin excitations is anticipated [6].

On the materials side, many of the ingredients needed for Kitaev magnetism have been identified in various iridates [7–11] and, more recently, α-$RuCl_3$ (hereafter $RuCl_3$) [12]. Several experimental and theoretical studies have established that $RuCl_3$ is a Mott insulator hosting spin-orbit coupled local moments [13–17]. Importantly, $RuCl_3$ displays a number of features characteristic of Kitaev magnetism. The magnetic interactions are highly anisotropic [18–20], and the system displays zigzag-type magnetic order with a small ordered moment below a T_N between 7 and 14 K, with the exact ordering temperature depending on the type of interlayer stacking [15,16,19]. The magnetic excitation spectra have also been interpreted in terms of Kitaev physics. Below T_N, the spin excitations observed in inelastic neutron scattering are reasonably accounted for with a minimal HK model [15] with a dominant K, while above T_N a broad continuum, reminiscent of the Kitaev QSL, is observed with neutron [15] and Raman scattering [21,22].

Despite these studies, the consequences of a dominant K are poorly understood, with the finite temperature properties of the HK and related models being a particular point of interest [23–29]. In particular, are aspects of the QSL phase manifested at finite temperatures in systems with a magnetically ordered ground state? Indeed, it has recently been predicted that the temperature dependence of several physical quantities, including the nearest-neighbor spin-spin correlations, may reveal signatures of the nearby QSL state [22,30]. Moreover, the relationship between spin and charge degrees of freedom, intensively studied in traditional Mott insulators [31–34], has not been extensively explored in this class of frustrated spin systems, although ultrafast optical studies have revealed anomalies in the photoexcited dynamics near T_N in some Ir-based materials [35,36].

With these issues in mind, we studied the optical properties of $RuCl_3$ over a broad temperature (T) range. Optical spectroscopy is a powerful tool for studying the charge dynamics in correlated electron matter [37] and can reveal changes in the electronic structure driven by spin or orbital ordering. We first argue that the optical response of $RuCl_3$ can be understood as intersite dd transitions within a multiorbital Hubbard model. These features exhibit a number of anomalies associated with magnetism, including a redistribution of spectral weight that we attribute to the development of short-ranged spin-spin correlations. The spin-spin correlations evolve over a broad temperature range ($>10T_N$) that is consistent with the highly frustrated, Kitaev-type interactions present in $RuCl_3$ [27]. We also find evidence for strong excitonic effects, including a quasibound excitonic state. Overall, our results provide an improved understanding of the relationship between spin and charge degrees of freedom in HK magnets.

II. EXPERIMENTAL METHODS AND RESULTS

We used spectroscopic ellipsometry to accurately measure the optical response of $RuCl_3$ from 4 to 300 K. Single crystals were prepared by vacuum sublimation of prereacted $RuCl_3$ powder [12]. The sample studied here contains a finite density of stacking faults and we expect some contribution from both the 7 and 14 K magnetic transitions in our data [38]. Any optical signatures of long-ranged order should occur near or below 14 K and so we take $T_N \sim 14$ K for simplicity. The temperature dependent optical properties of a $\sim 1.5 \times 1.5 \times 0.1$ mm^3 single crystal were measured using a Woollam VASE

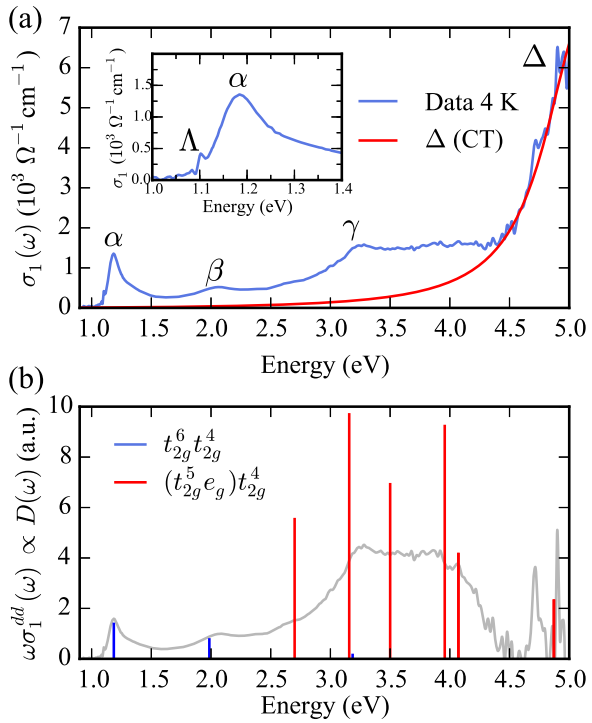

FIG. 1. Optical response of $RuCl_3$. (a) Real part of the optical conductivity $\sigma_1(\omega)$ at 4 K. The red line indicates the Cl p to Ru d charge transfer contribution. Inset: low energy detail of $\sigma_1(\omega)$. (b) Optical joint density of states $D(\omega)$ vs the results of the multiplet calculation.

spectroscopic ellipsometer equipped with an optical cryostat. The sample was first cooled to base temperature and the spectra were collected on warming. Throughout the measurement, the pressure in the sample chamber was kept at 2.1×10^{-9} mbar or below to avoid icing. The spectral resolution was set to 2 (20) meV in the range 0.9 to 1.4 (1.4 to 5.0) eV and the optical data was collected from a cleaved, ab surface at a 70° angle of incidence. The complex optical conductivity $[\hat{\sigma}(\omega)]$ was directly derived from the ellipsometric data.

The real part of the optical conductivity $[\sigma_1(\omega)]$ at 4 K is shown in Fig. 1(a). Consistent with earlier reports [14,39], four main features are visible in $\sigma_1(\omega)$ near 1.2, 2.1, 3.2, and 5.0 eV, which we label α, β, γ, and Δ [Fig. 1(a)]. As we shall explain in more detail below, the α, β, and γ features correspond to intersite $d^5d^5 \rightarrow d^4d^6$ transitions involving Ru t_{2g} and e_g states. Meanwhile, the comparatively intense Δ is a Cl p to Ru d charge transfer excitation. The optical gap, which corresponds to the onset of α, is about 1 eV [14].

The $\sigma_1(\omega)$ spectrum shown in Fig. 1(a) reveals signatures of strong excitonic (i.e., final state electron-hole interaction) effects. The asymmetric and narrow line shape of α is reminiscent of the excitations observed in some 1D and 2D materials where excitonic effects are thought to be strong [40,41]. Further evidence for excitonic effects is provided in the inset to Fig. 1(a), where a sharp resonance (Λ) is seen just above the gap which can be interpreted as a bound excitonic state [42]. A recent photoemission study reported a charge gap of at least 1.2 eV, which also suggests that $\sigma_1(\omega)$ is significantly renormalized by electron-hole interactions [43]. Finally, a comparison with published photoconductivity data also points to the sizable excitonic character of the optical absorption edge and can be found in the Appendix.

A. Multiorbital Hubbard model for $\sigma_1(\omega)$

The three peaks α, β, and γ in $\sigma_1(\omega)$ [Fig. 1(a)] are a result of the multiplet structure of the photoexcited d^4d^6 states, which is determined by the effective Hubbard parameter (U_{eff}), Hund's coupling (J_H), and the crystal electric field ($10Dq$) [44,45]. To illustrate how multiplet effects determine $\sigma_1(\omega)$, we evaluated the dd contribution to the optical response using a simple cluster model for the photoexcited states. We computed the energies and degeneracies of the photoexcited states using standard expressions [45], enforcing the spin selection rule but ignoring spin-orbit coupling and matrix element (hopping) effects. The parameters U_{eff}, $10Dq$, and J_H were set to 2.386, 2.2, and 0.4 eV, respectively, consistent with earlier work [14]. Note that U_{eff}, which includes excitonic effects implicitly, is chosen such that the lowest energy excited state coincides with α and is the only free parameter: $10Dq$ and J_H are fixed by other measurements [14]. We ignored spin-orbit coupling effects in the excited states as $\lambda \sim 0.1$ eV is small compared to the other energy scales. Further details are included in the Appendix.

The results of our cluster model calculation are presented in Fig. 1(b), together with the dd optical joint density of states $D(\omega) \propto \omega\sigma_1^{dd}(\omega)$ [46] obtained from $\sigma_1(\omega)$ after subtracting the charge transfer component Δ [red line in Fig. 1(a)]. The calculated optical response is shown as lines, with the length of each line indicating the degeneracy of the states at that energy times an overall scaling factor chosen to match the intensity of α. Remarkably, the main features of $D(\omega)$ are satisfactorily reproduced, despite the simplicity of our approach. In particular, the three peak structure, corresponding to α, β, and γ, the relative intensities of α and β, and the overall bandwidth and line shape of γ are all replicated in the calculation. We speculate that the success of the cluster calculation may be partially explained by the strong excitonic effects discussed earlier, as these would be expected to reduce the bandwidth of the photoexcited states. We also mention that a cluster calculation approach provides a good account of $\sigma_1(\omega)$ and other spectroscopic data for the related material Na_2IrO_3 [47].

Comparison with the model result allows us to assign α and β to $t_{2g}^4 t_{2g}^6$ excitations, while γ clearly arises from $t_{2g}^4(t_{2g}^5 e_g)$ excited states. The $t_{2g}^4 t_{2g}^6$ excitations are further split according to the multiplet structure of the t_{2g}^4 ion, yielding α ($E = U_{\mathrm{eff}} - 3J_H$) and β ($E = U_{\mathrm{eff}} - J_H$). An additional weak $t_{2g}^4 t_{2g}^6$ excitation ($E = U_{\mathrm{eff}} + 2J_H$) is also expected but is not resolved in the data. The intensity of the $t_{2g}^4(t_{2g}^5 e_g)$ peak γ is overestimated by approximately a factor of 2, likely due to the different matrix elements (hopping terms) for $t_{2g} \rightarrow t_{2g}$ and $t_{2g} \rightarrow e_g$ processes.

B. Temperature dependence of $\sigma_1(\omega)$

To investigate possible connections between the charge dynamics and magnetism, we now turn to the T-dependent $\sigma_1(\omega)$ spectra, shown in Fig. 2(a) for representative temperatures. The spectra of Fig. 2(a) reveal a strong

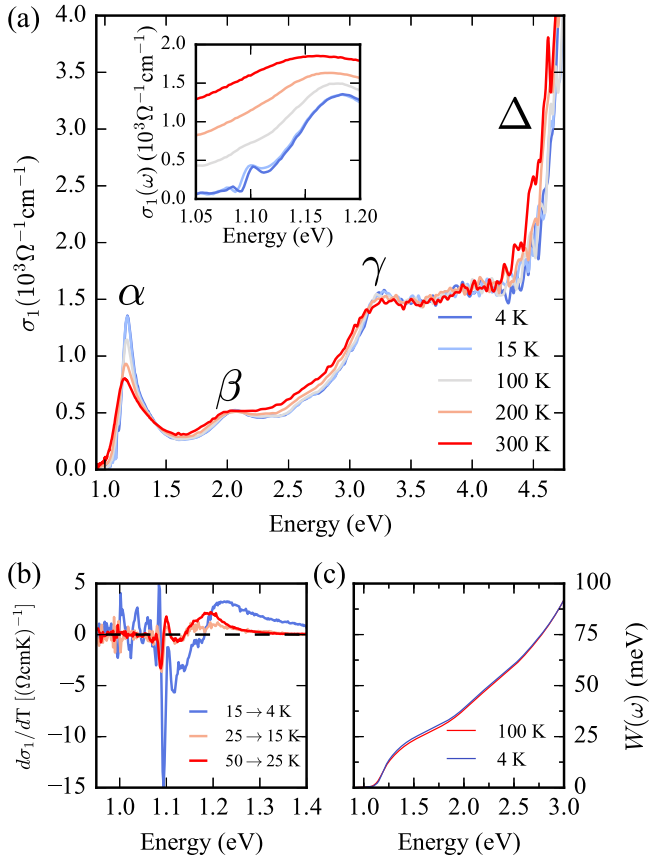

FIG. 2. T-dependent optical properties of $RuCl_3$. (a) $\sigma_1(\omega)$ at representative T. Inset: low energy detail of Λ and α. The 100, 200, and 300 K data are offset for clarity in the inset. (b) Difference spectra $d\sigma_1(\omega)/dT$ over different T intervals. (c) Energy-dependent spectral weight $W(\omega)$ at 100 and 4 K.

temperature dependence that is suggestive of many-body effects. As T is increased, α broadens and loses intensity. Meanwhile, β, γ, and Δ redshift and broaden as T is raised above $\sim$ 100 K. A well-defined isosbestic point is visible near 1.42 eV, indicating a transfer of spectral weight from low to high energies as T increases. The Λ resonance also displays a strong temperature dependence, redshifting and broadening as T is raised and is difficult to discern in the data above 100 K [inset to Fig. 2(a)]. Finally, the change of the optical gap is minimal ($\sim$ 0.1 eV over the full temperature range), consistent with a well-developed Mott insulating state.

Magnetic order produces clear anomalies in the T dependence of $\sigma_1(\omega)$. This is best appreciated by considering the difference spectra $d\sigma_1/dT = [\sigma_1(T_{\mathrm{low}}) - \sigma_1(T_{\mathrm{high}})]/(T_{\mathrm{high}} - T_{\mathrm{low}})$ displayed in Fig. 2(b). Between 50 and 25 K, $d\sigma_1/dT$ shows a broad dip-peak structure, with a sharper feature due to Λ near 1.1 eV. The overall line shape of the difference spectra suggest both a blueshift and spectral weight increase of α and Λ as T decreases. Qualitatively similar behavior is observed between 25 and 15 K, although the magnitude of $d\sigma_1/dT$ is reduced. In contrast, relatively rapid changes in $\sigma_1(\omega)$ occur between 15 and 4 K. Clearly, $d\sigma_1/dT$ is significantly larger across T_N, although the overall line shape is similar to that observed at higher temperatures. The excitonic resonance Λ and α are both affected by long ranged order and blueshift by $\sim$ 2 meV [inset of Fig. 2(a)]. The comparatively large changes in $\sigma_1(\omega)$ near T_N indicate a coupling between the high-energy charge dynamics and magnetism.

The isosbestic point visible in Fig. 2(a) indicates that a transfer of spectral weight into α also occurs as T is reduced. To examine the spectral weight transfer in more detail, we consider the integrated spectral weight $W(\omega) = \frac{2\hbar a_o}{\pi e^2}\int_{0.93}^{\omega}\sigma_1(\omega')d\omega'$ [48]. Here $W(\omega)$ is expressed as a kinetic energy and the Ru-Ru distance $a_o = 3.4$ Å. The resulting $W(\omega)$ are shown in Fig. 2(c) at 4 and 100 K. At both temperatures, $W(\omega)$ is negligible below the gap near 1 eV before rising rapidly due to α. At this point, the $W(4\ \mathrm{K},\omega)$ curve is slightly larger than $W(100\ \mathrm{K},\omega)$, meaning the spectral weight of α is increased at 4 K compared to 100 K. The two curves then gradually merge and the total spectral weight is conserved below $\sim$ 3 eV. This suggests that spectral weight is transferred to α from β and/or γ as T is reduced. The energy scale ($\sim$ 1.8 eV) of the spectral weight redistribution (Fig. 2) is large, suggesting electron-electron interactions, and in fact closely corresponds to the $5J_H \sim 2.0$ eV spread expected for the $t_{2g}^4 t_{2g}^6$ excitations [Fig. 1(b)].

III. SPECTRAL WEIGHT AND SPIN-SPIN CORRELATIONS

The spectral weight redistribution evident in Fig. 2(c) may be ascribed to the development of the nearest-neighbor (nn) spin-spin correlations. In a Mott insulator, the intensities of intersite dd transitions are known to provide insight into the nn spin-spin correlations [31,32,49–52]. Following the optical sum rule for tight-binding models, the spectral weight of the dd transitions in $\sigma_1(\omega)$ may be associated with the kinetic energy of the virtual charge fluctuations that contribute to superexchange [53]. For magnetic ions i and j separated by distance a_o, this relationship may be stated formally in terms of the partial sum rule [33]:

$$\frac{\pi}{2}W_m = \frac{a_o\hbar}{e^2}\int_0^{\infty}\sigma_1^{(m)}(\omega)d\omega = -\pi\langle H_m(ij)\rangle. \qquad (1)$$

Here W_m is the kinetic energy associated with virtual charge fluctuations along the bond direction to excited state m, while $\sigma_1^{(m)}$ is the contribution of excited state m to $\sigma_1(\omega)$ for polarization along the bond direction. Lastly, $\langle H_m(ij)\rangle$ is the superexchange energy for bond (i,j) associated with m.

The partial sum rule [Eq. (1)] suggests that $\sigma_1(\omega)$ should reveal signatures of the novel magnetic correlations present in $RuCl_3$, as the multiplet structure of the photoexcited states is clearly resolved in our optical data [α, β, and γ in Fig. 1(a)]. Within a minimal HK model for $RuCl_3$, $H(ij) = K S_i^{\gamma} S_j^{\gamma} + J\vec{S}_i\cdot\vec{S}_j$ [15], where γ depends on the specific bond direction and $\vec{S}_i$ describes the spin at site i [54]. A straightforward application of Eq. (1) then yields

$$W_m/2 = -K_m\langle S_i^{\gamma} S_j^{\gamma}\rangle - J_m\langle\vec{S}_i\cdot\vec{S}_j\rangle, \qquad (2)$$

with the coefficients K_m and J_m determined by the hopping between Ru d states and the energy of excited state m [4,13,33]. We note that the $t_{2g}^4(t_{2g}^5 e_g)$ excitations are located at relatively large energies ($>$ 2.7 eV) and are weakly T dependent, which

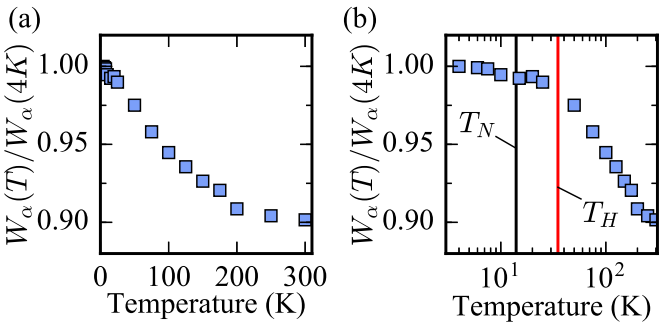

FIG. 3. Temperature-dependent spectral weight W_α on (a) linear and (b) semilogarithmic scales. The magnetic ordering temperature T_N and the crossover scale T_H are indicated in (b).

indicates that these transitions may not strongly contribute to the magnetic interactions.

To examine the T dependence of the spectral weight in detail, we now focus on $W_\alpha = \frac{2\hbar a_o}{\pi e^2}\int_{0.93}^{1.42}\sigma_1(\omega)d\omega$, where the integral runs from below the optical gap up to the isosbestic point at 1.42 eV. The resulting W_α is shown in Figs. 3(a) and 3(b) normalized to the 4 K value. Starting from 300 K, W_α rises monotonically as T is reduced. At lower temperatures, W_α increases more rapidly before saturating near 25 K. Below T_N, W_α displays a further increase [Fig. 3(b)], although this is small compared to the overall change in W_α. However, we do not observe a clear saturation of W_α at the (nominal) base temperature of 4 K and so our data do not rule out the possibility of a further increase of W_α at lower T. Overall, the data suggest that W_α, and by extension the *nn* spin-spin correlations, exhibit significant temperature dependence up to at least $\sim 10T_N$, indicating highly frustrated magnetic interactions. This is consistent with other probes of the magnetism: the magnetic susceptibility deviates from the Curie-Weiss form near 140 K [19], while the magnetic entropy begins to drop near the same temperature and is mostly exhausted above T_N [20].

The variation of W_α with T is compatible with theoretical expectations for the Kitaev model and with other estimates for the magnetic interaction energy scale. Studies of the Kitaev model using both quantum Monte Carlo and cluster DMFT methods have shown that the bond-dependent spin-spin correlation $\langle S_i^\gamma S_j^\gamma\rangle$ develops gradually according to the crossover scale $T_H \sim 0.375\ K$ [27,55]. For $T < T_H$, $\langle S_i^\gamma S_j^\gamma\rangle$ is weakly T dependent. At $T \sim T_H$, $\langle S_i^\gamma S_j^\gamma\rangle$ begins to decrease before smoothly crossing over to Curie-Weiss behavior at $T >> T_H$. Qualitatively similar behavior is evident in W_α [Fig. 3(b)]. By comparing our data with the theoretical results (Fig. 1(b) of Ref. [55]), we can estimate $T_H \sim 35$ K [red line in Fig. 3(b)], which corresponds to $|K| \sim 8$ meV, in good agreement with other experimental estimates, which range from 7 to 10 meV [15,21,22]. The similarity between $\langle S_i^\gamma S_j^\gamma\rangle$ from theory and $W_\alpha(T)$ may be due to a dominant K and/or K_α [i.e., $K_\alpha\langle S_i^\gamma S_j^\gamma\rangle >> J_\alpha\langle\vec{S}_i\cdot\vec{S}_j\rangle$ in Eq. (2)].

The temperature dependence of $W_\alpha(T)$ should be contrasted with the behavior established for unfrustrated spin systems. Typically, large variations in spectral weight are only expected in the vicinity of T_N [49]. An established example would be $CeVO_3$ [56], where changes in spectral weight occur at T_N but are almost negligible at higher T. In fact, our observations in $RuCl_3$ are reminiscent of the frustrated, one-dimensional spin system $LiCuVO_4$ [50], where a gradual temperature dependence of the spectral weight is observed far above T_N. Unfortunately, we are not aware of optical data for an unfrustrated, 2D honeycomb lattice material that would constitute the best comparison for $RuCl_3$.

The fractional 10% change in W_α from high to low T is modest compared to many other materials (cf., the $CeVO_3$ data reported in Ref. [56]), which may be due to the comparatively small spin-spin correlations achieved by the frustrated magnetic interactions in $RuCl_3$. In the pure Kitaev limit, the bond-dependent *nn* spin-spin correlations should reach 0.125 [27], compared with the fully polarized case of 0.25. Moreover, a recent *ab initio* plus exact diagonalization study of $RuCl_3$ that included magnetic interactions beyond the Kitaev term found that even in the zigzag ordered state the *nn* correlations are still only in the range 0.05 to 0.1 [57]. Thus we expect the change in W_α to be reduced compared to systems where larger spin-spin correlations are achieved. A second possible explanation is more prosaic: the experimental W_α likely contains contributions from the tails of β and γ that are less T dependent.

The above analysis indicates that the T-dependent optical response of $RuCl_3$ may be consistently understood in terms of *dd* excitations within a multiorbital Hubbard model with frustrated Kitaev-type interactions. However, we emphasize that the optical data alone does not provide evidence for a dominant K: qualitatively similar behavior would be expected for other types of frustrated interactions and so we rely on other studies for this point. The role of the subdominant magnetic couplings in the optical data, such as the Heisenberg term J, also remains to be clarified. Proper consideration of the subdominant interactions is essential to capture the long-range order and other aspects of the magnetism. We expect that, in terms of the optical data presented here, inclusion of subdominant magnetic interactions may be needed to account for the increase of W_α at T_N and may also affect the assumed relationship between the crossover temperature T_H and K.

IV. CONCLUSIONS

In summary, we have investigated the connection between $\sigma_1(\omega)$ and magnetism in the HK magnet $RuCl_3$. As T is reduced, we observe a transfer of spectral weight from high to low energies due to *nn* spin correlations that develop far above T_N, consistent with highly frustrated magnetic interactions. The temperature dependence of these correlations agrees with theoretical expectations for the HK model with an energy scale suitable to $RuCl_3$. The $\sigma_1(\omega)$ spectra also show evidence for strong excitonic effects, including a bound state.

ACKNOWLEDGMENTS

We thank Y. Motome, J. Knolle, S. Sinn, K. S. Burch, and B. H. Kim for helpful comments. This work was supported by the Institute for Basic Science in Korea (Grant No. IBS-R009-D1) and by the Basic Science Research Program through the National Research Foundation of Korea (NRF)

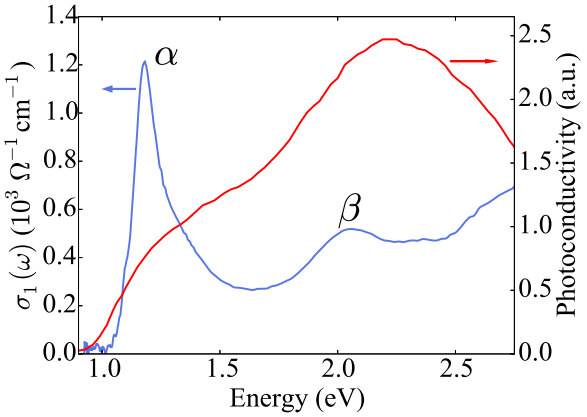

FIG. 4. Optical conductivity and photoconductivity of $RuCl_3$. The optical conductivity was measured at 75 K, while the photoconductivity is reproduced from Ref. [39] and was collected at 80 K.

funded by the Ministry of Science, ICT, and Future Planning (NRF-2015R1A2A1A10056200). Work at the University of Toronto was supported by the National Sciences and Engineering Research Council (NSERC) of Canada through the Collaborative Research and Training Experience (CREATE) program and a Discovery Grant.

APPENDIX A: EXCITONIC EFFECTS IN $\sigma_1(\omega)$ AND PHOTOCONDUCTIVITY

The importance of excitonic effects may be gauged by comparing the optical conductivity [$\sigma_1(\omega)$] with the photoconductivity [40]. This comparison indicates sizable excitonic effects in $RuCl_3$, but that the α peak is not a true bound state. In Fig. 4, $\sigma_1(\omega)$ measured at 75 K is plotted along with published 80 K photoconductivity data (Binnotto *et al.*, Ref. [39]). The principle features of $\sigma_1(\omega)$ are described in the main text. The photoconductivity data shows an onset near 1 eV and continues to increase with increasing photon energy up to a broad peak near 2.2 eV. Two important points are evident in Fig. 4. The first point is that the photoconductive response rises rather gradually above the 1 eV onset. Indeed, the photoconductive response at 1.18 eV (the α peak position) is only 31% of the maximum value. In contrast, for the limiting case of negligible excitonic effects, we expect that the photoconductivity should resemble a step function. The suppression of the near gap photoconductive response can be explained by significant electron-hole interaction effects [40]. The second point is that the onset in the photoconductivity is located *below* the gap in $\sigma_1(\omega)$. This indicates that delocalized, charged excitations exist at the optical absorption edge, despite the strong excitonic character. Overall, the data shown in Fig. 4 reveal sizable excitonic effects. This is qualitatively consistent with the Λ resonance and the asymmetric line shape of α discussed in the main text. In a Mott insulator, the relevance of excitonic effects is to first approximation determined by the ratio of the nearest-neighbor Coulomb interaction (V) to the bandwidth [42]. In $RuCl_3$, V might be expected to be large due to the extended nature of the $4d$ orbitals. This may explain the apparent importance of excitonic effects in $RuCl_3$.

TABLE I. Ru d^6 states. The orbital, spin, and total degeneracies are labeled as l, s, and g, respectively.

State	l	s	g
$^1A_1$	1	1	1
$^3T_1$	3	3	9
$^3T_2$	3	3	9
$^1T_1$	3	1	3
$^1T_2$	3	1	3

TABLE II. Ru ion d^4 states. The orbital, spin, and total degeneracies are labeled as l, s, and g, respectively.

State	l	s	g
$^3T_1$	3	3	9
$^1T_2$	3	1	3
^1E_v	1	1	1
^1E_u	1	1	1
$^1A_1$	1	1	1

APPENDIX B: MULTIPLET STRUCTURE OF THE d^4d^6 EXCITED STATE

To understand the multipeak structure evident in $\sigma_1(\omega)$, we consider the multiplet structure of the photoexcited d^4d^6 state following the procedure outlined in Ref. [45]. We considered excited states with energies $E(M_{d^4}, M_{d^6}) = E(M_{d^4}) + E(M_{d^6}) - 2E(^2T_2)$, where M_{d^4} (M_{d^6}) refers to a specific multiplet state of the d^4 (d^6) ion. The d^5 ground state is taken to be the low-spin $^2T_2$. For the excited d^4 (d^6) ion, we considered the $^3T_1$,$^1T_2$,^1E_u,^1E_v, and $^1A_1$ ($^1A_1$,$^3T_1$,$^3T_2$,$^1T_1$, and $^1T_2$) states. The relevant states, as well as their spin (s), orbital (l), and total (g) degeneracies are listed in Tables I and II for the d^4 and d^6 ions, respectively. The photoexcited states and their degeneracies can be computed from these tables. The resulting $t_{2g}^4 t_{2g}^6$ excited states are shown in Table III along with their energies (E) and number of states with total spin 0 or 1 (N). The ground state of the d^5 ion is the low spin $^2T_2$ so a pair of Ru ions in the ground state can have a total spin of 0 or 1 which is conserved in the optical excitation process. The energies (E) are given in terms of the effective Hubbard parameter (U_{eff}), the cubic crystal electric field ($10Dq$), and the Hund's coupling (J_H), which we set to 2.386, 2.2, and 0.4 eV, respectively. Tables IV and V list the excited states for $t_{2g}^4(t_{2g}^5 e_g)$ excitations. We have only tabulated states whose energies fall in our experimental range. In Fig. 1(b) of the main text, these transitions are represented by a vertical line at E whose height is given by N.

TABLE III. Possible $t_{2g}^4 t_{2g}^6$ excited states (d^6:$^1A_1$). The energy and number of photoexcited states are labeled E and N, respectively.

d^4	N	E
$^3T_1$	9	$U_{\text{eff}} - 3J_H$
$^1T_2$	3	$U_{\text{eff}} - J_H$
^1E_v	1	$U_{\text{eff}} - J_H$
^1E_u	1	$U_{\text{eff}} - J_H$
$^1A_1$	1	$U_{\text{eff}} + 2J_H$

TABLE IV. Possible $t_{2g}^4(t_{2g}^5 e_g)$ excited states (d^4:$^3T_1$). The energy and number of photoexcited states are labeled E and N, respectively.

d^6	N	E
$^3T_2$	36	$U_{\text{eff}} - \frac{33}{7}J_H + 10Dq$
($^3T_1$,$^1T_2$)	63	$U_{\text{eff}} - \frac{25}{7}J_H + 10Dq$
$^1T_1$	27	$U_{\text{eff}} - \frac{9}{7}J_H + 10Dq$

TABLE V. Possible $t_{2g}^4(t_{2g}^5 e_g)$ excited states (d^4 : [$^1T_2$,^1E_u ,^1E_v]). The $^1T_2$, ^1E_u, and ^1E_v states of the d^4 ion are degenerate in our model and so we group them together here.

d^6	N	E
$^3T_2$	45	$U_{\text{eff}} - \frac{19}{7}J_H + 10Dq$
($^3T_1$,$^1T_2$)	60	$U_{\text{eff}} - \frac{11}{7}J_H + 10Dq$
$^1T_1$	15	$U_{\text{eff}} + \frac{5}{7}J_H + 10Dq$

[1] L. Balents, Nature (London) **464**, 199 (2010).
[2] J. Chaloupka, G. Jackeli, and G. Khaliullin, Phys. Rev. Lett. **105**, 027204 (2010).
[3] G. Jackeli and G. Khaliullin, Phys. Rev. Lett. **102**, 017205 (2009).
[4] J. G. Rau, E. K.-H. Lee, and H.-Y. Kee, Phys. Rev. Lett. **112**, 077204 (2014).
[5] I. Rousochatzakis, J. Reuther, R. Thomale, S. Rachel, and N. B. Perkins, Phys. Rev. X **5**, 041035 (2015).
[6] A. Kitaev, Ann. Phys. (N.Y.) **321**, 2 (2006).
[7] Y. Singh and P. Gegenwart, Phys. Rev. B **82**, 064412 (2010).
[8] H. Gretarsson, J. P. Clancy, X. Liu, J. P. Hill, E. Bozin, Y. Singh, S. Manni, P. Gegenwart, J. Kim, A. H. Said, D. Casa, T. Gog, M. H. Upton, H.-S. Kim, J. Yu, V. M. Katukuri, L. Hozoi, J. van den Brink, and Y.-J. Kim, Phys. Rev. Lett. **110**, 076402 (2013).
[9] Y. Singh, S. Manni, J. Reuther, T. Berlijn, R. Thomale, W. Ku, S. Trebst, and P. Gegenwart, Phys. Rev. Lett. **108**, 127203 (2012).
[10] T. Takayama, A. Kato, R. Dinnebier, J. Nuss, H. Kono, L. S. I. Veiga, G. Fabbris, D. Haskel, and H. Takagi, Phys. Rev. Lett. **114**, 077202 (2015).
[11] V. M. Katukuri, S. Nishimoto, V. Yushankhai, A. Stoyanova, H. Kandpal, S. Choi, R. Coldea, I. Rousochatzakis, L. Hozoi, and J. van den Brink, New J. Phys. **16**, 013056 (2014).
[12] K. W. Plumb, J. P. Clancy, L. J. Sandilands, V. Vijay Shankar, Y. F. Hu, K. S. Burch, H.-Y. Kee, and Y.-J. Kim, Phys. Rev. B **90**, 041112(R) (2014).
[13] H.-S. Kim, Vijay Shankar V., A. Catuneanu, and H.-Y. Kee, Phys. Rev. B **91**, 241110(R) (2015).
[14] L. J. Sandilands, Y. Tian, A. A. Reijnders, H.-S. Kim, K. W. Plumb, Y.-J. Kim, H.-Y. Kee, and K. S. Burch, Phys. Rev. B **93**, 075144 (2016).
[15] A. Banerjee, C. A. Bridges, J.-Q. Yan, A. A. Aczel, L. Li, M. B. Stone G. E. Granroth, M. D. Lumsden, Y. Yiu, J. Knolle *et al.*, Nat. Mater. **15**, 733 (2016).
[16] R. D. Johnson, S. C. Williams, A. A. Haghighirad, J. Singleton, V. Zapf, P. Manuel, I. I. Mazin, Y. Li, H. O. Jeschke, R. Valentí, and R. Coldea, Phys. Rev. B **92**, 235119 (2015).
[17] B. H. Kim, T. Shirakawa, and S. Yunoki, Phys. Rev. Lett. **117**, 187201 (2016).
[18] M. Majumder, M. Schmidt, H. Rosner, A. A. Tsirlin, H. Yasuoka, and M. Baenitz, Phys. Rev. B **91**, 180401 (2015).
[19] J. A. Sears, M. Songvilay, K. W. Plumb, J. P. Clancy, Y. Qiu, Y. Zhao, D. Parshall, and Y.-J. Kim, Phys. Rev. B **91**, 144420 (2015).
[20] Y. Kubota, H. Tanaka, T. Ono, Y. Narumi, and K. Kindo, Phys. Rev. B **91**, 094422 (2015).
[21] L. J. Sandilands, Y. Tian, K. W. Plumb, Y.-J. Kim, and K. S. Burch, Phys. Rev. Lett. **114**, 147201 (2015).
[22] J. Nasu, J. Knolle, D. L. Kovrizhin, Y. Motome, and R. Moessner, Nat. Phys. **12**, 912 (2016).
[23] C. C. Price and N. B. Perkins, Phys. Rev. Lett. **109**, 187201 (2012).
[24] C. Price and N. B. Perkins, Phys. Rev. B **88**, 024410 (2013).
[25] J. Reuther, R. Thomale, and S. Trebst, Phys. Rev. B **84**, 100406 (2011).
[26] J. Nasu, M. Udagawa, and Y. Motome, Phys. Rev. Lett. **113**, 197205 (2014).
[27] J. Nasu, M. Udagawa, and Y. Motome, Phys. Rev. B **92**, 115122 (2015).
[28] J. Nasu and Y. Motome, Phys. Rev. Lett. **115**, 087203 (2015).
[29] M. Hermanns, S. Trebst, and A. Rosch, Phys. Rev. Lett. **115**, 177205 (2015).
[30] Y. Yamaji, T. Suzuki, T. Yamada, S.-i. Suga, N. Kawashima, and M. Imada, Phys. Rev. B **93**, 174425 (2016).
[31] N. N. Kovaleva, A. V. Boris, C. Bernhard, A. Kulakov, A. Pimenov, A. M. Balbashov, G. Khaliullin, and B. Keimer, Phys. Rev. Lett. **93**, 147204 (2004).
[32] M. W. Kim, Y. S. Lee, T. W. Noh, J. Yu, and Y. Moritomo, Phys. Rev. Lett. **92**, 027202 (2004).
[33] G. Khaliullin, P. Horsch, and A. M. Oleś, Phys. Rev. B **70**, 195103 (2004).
[34] B. H. Kim, G. Khaliullin, and B. I. Min, Phys. Rev. Lett. **109**, 167205 (2012).
[35] Z. Alpichshev, F. Mahmood, G. Cao, and N. Gedik, Phys. Rev. Lett. **114**, 017203 (2015).
[36] J. P. Hinton, S. Patankar, E. Thewalt, A. Ruiz, G. Lopez, N. Breznay, A. Vishwanath, J. Analytis, J. Orenstein, J. D. Koralek, and I. Kimchi, Phys. Rev. B **92**, 115154 (2015).
[37] D. N. Basov, R. D. Averitt, D. van der Marel, M. Dressel, and K. Haule, Rev. Mod. Phys. **83**, 471 (2011).
[38] H. B. Cao, A. Banerjee, J.-Q. Yan, C. A. Bridges, M. D. Lumsden, D. G. Mandrus, D. A. Tennant, B. C. Chakoumakos, and S. E. Nagler, Phys. Rev. B **93**, 134423 (2016).
[39] L. Binotto, I. Pollini, and G. Spinolo, Phys. Status Solidi B **44**, 245 (1971).
[40] M. Ono, K. Miura, A. Maeda, H. Matsuzaki, H. Kishida, Y. Taguchi, Y. Tokura, M. Yamashita, and H. Okamoto, Phys. Rev. B **70**, 085101 (2004).
[41] J. P. Falck, A. Levy, M. A. Kastner, and R. J. Birgeneau, Phys. Rev. Lett. **69**, 1109 (1992).

[42] K. W. Kim, G. D. Gu, C. C. Homes, and T. W. Noh, Phys. Rev. Lett. **101**, 177404 (2008).
[43] X. Zhou, H. Li, J. A. Waugh, S. Parham, H.-S. Kim, J. A. Sears, A. Gomes, H.-Y. Kee, Y.-J. Kim, and D. S. Dessau, Phys. Rev. B **94**, 161106(R) (2016).
[44] T. Katsufuji, T. Takubo, and T. Suzuki, Phys. Rev. B **87**, 054424 (2013).
[45] J. S. Lee, M. W. Kim, and T. W. Noh, New J. Phys. **7**, 147 (2005).
[46] M. Dressel and G. Grüner, *Electrodynamics of Solids: Optical Properties of Electrons in Matter* (Cambridge University Press, Cambridge, 2002).
[47] B. H. Kim, G. Khaliullin, and B. I. Min, Phys. Rev. B **89**, 081109 (2014).
[48] M. M. Qazilbash, A. A. Schafgans, K. S. Burch, S. J. Yun, B. G. Chae, B. J. Kim, H. T. Kim, and D. N. Basov, Phys. Rev. B **77**, 115121 (2008).
[49] C. Taranto, G. Sangiovanni, K. Held, M. Capone, A. Georges, and A. Toschi, Phys. Rev. B **85**, 085124 (2012).
[50] Y. Matiks, P. Horsch, R. K. Kremer, B. Keimer, and A. V. Boris, Phys. Rev. Lett. **103**, 187401 (2009).
[51] A. M. Oleś, G. Khaliullin, P. Horsch, and L. F. Feiner, Phys. Rev. B **72**, 214431 (2005).
[52] Y. Motome, H. Seo, Z. Fang, and N. Nagaosa, Phys. Rev. Lett. **90**, 146602 (2003).
[53] K. H. Ahn and A. J. Millis, Phys. Rev. B **61**, 13545 (2000).
[54] We ignore other possible interactions, such as the so-called Γ term, for simplicity.
[55] J. Yoshitake, J. Nasu, and Y. Motome, Phys. Rev. Lett. **117**, 157203 (2016).
[56] J. Reul, A. A. Nugroho, T. T. M. Palstra, and M. Grüninger, Phys. Rev. B **86**, 125128 (2012).
[57] R. Yadav, N. A. Bogdanov, V. M. Katukuri, S. Nishimoto, J. van den Brink, and L. Hozoi, arXiv:1604.04755 [cond-mat.str-el].